Characterization of two types of cesium-bearing microparticle (CsMP) emitted from the Fukushima nuclear power plant accident using multiple synchrotron radiation analyses

On March 11, 2011, a great earthquake hit the eastern part of mainland Japan and triggered several gigantic tsunami waves that attacked the six-unit Fukushima Daiichi Nuclear Power Plant (FDNPP). The tsunamis damaged the electric functions to cool reactor cores and rapidly increased the temperature in the primary containment vessels, finally resulting in accidents in Units 1–3. As a result, large amounts of radionuclides in the nuclear reactors of FDNPP were released into the environment [1]. Ten years after the accident, the internal conditions of these units are still unknown.

Some of the radiocesium (Cs) emitted by the Fukushima nuclear accident was incorporated in Cs-bearing microparticles (CsMPs) mainly consisting of silica (SiO_2) [2]. There have been mainly two types of CsMP found thus far. One is called Type-A CsMP, which is spherical with a diameter of ~0.1–10 μm and ~10^{-2}–10^{2} Bq ^{137}Cs radioactivity per particle, and was emitted from Unit 2 or 3 of FDNPP. In contrast, Type-B CsMP has various shapes of 50–400 μm diameter and 10^{1}–10^{4} ^{137}Cs (Bq/particle), and was emitted from Unit 1. The chemical properties of these radioactive particles have been reported in detail, but in the previous studies, only a small number of particles were investigated especially in the case of Type-B CsMPs. In this study, we endeavored to understand the radioactive particles systematically by analyzing a large number of particles [3]. In particular, micro-X-ray computed tomography (X-ray μ-CT) combined with X-ray fluorescence (XRF) analysis played an important role in analyzing these samples because of the presence of many voids and an iron (Fe)-rich part within the Type-B CsMPs [3].

As for CsMPs, road dust samples and other materials were collected at more than 100 sites within 50 km of FDNPP during 2011-2012. Sixty-seven CsMP samples were isolated in three steps [3]. First, the spatial distribution of radioactive Cs in the samples was measured by autoradiography with imaging plates to identify CsMPs. Second, the wet separation method [4-6] was employed to isolate CsMPs from the samples containing CsMPs. After the isolation, the CsMP in water used for the separation was carefully dropped on Kapton tape and air-dried for scanning electron microscopy (SEM) with energy-dispersive spectrometer (EDS) analysis to finally identify CsMPs on the basis of shape and elemental composition. For Type-B CsMPs, X-ray μ-CT analysis was conducted at SPring-8 **BL37XU** [3]. We could acquire projection images at different angles that included information on the inner structure. Element maps were also generated by observing the difference between the pre-edge and post-edge energies of the element. In this study, projections below and above Fe and zinc (Zn) *K*-edges were recorded to obtain Fe and Zn maps. For the Type-B CsMPs, 2D μ-XRF measurement for various elements was conducted at BL-4A of the Photon Factory, KEK.

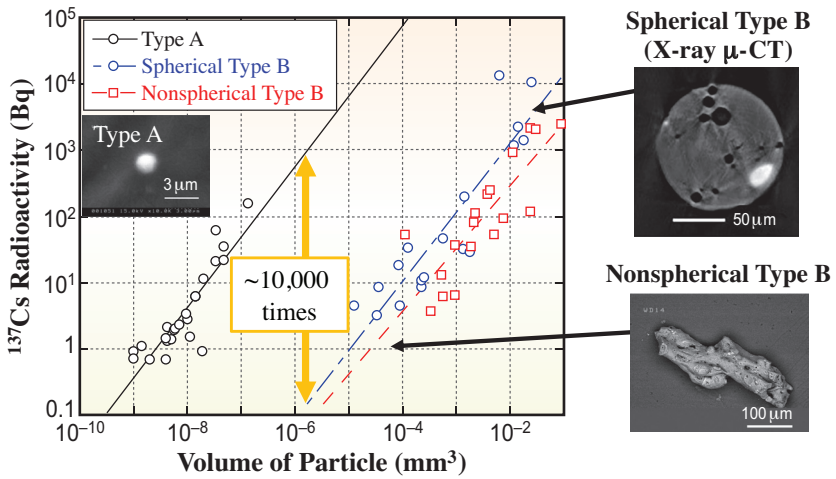

Fig. 1. Relationship between ^{137}Cs radioactivity and volume of each CsMP with X-ray μ-CT image for spherical Type-B CsMP.

X-ray μ-CT results for Type-B CsMPs show a number of voids in their structures possibly related to gas release during their cooling processes. A CT image for one sample of Type-B CsMP is shown in Fig. 1. White areas in the CT image absorbed X-rays to a greater degree than the matrix area, reflecting the presence of heavy elements in Type-B CsMPs. Although it is difficult to determine the volume of Type-B CsMPs from the external shape, X-ray μ-CT analysis enabled us to accurately calculate the volume of internal voids. On the other hand, the volume of Type-A CsMPs was calculated from the apparent diameter, since we can assume a spherical shape on the basis of transmission electron microscopy (TEM) observations reported thus far [2]. Figure 1 shows the relationship between ^{137}Cs radioactivity and volume for Types-A and -B CsMPs. As a result, the ^{137}Cs concentration per volume (Bq/mm^3) of Type-A CsMPs was ~10,000 times higher than that of Type-B CsMPs. Among the Type-B CsMPs, the spherical ones had higher concentrations of volatile elements such as ^{137}Cs than the nonspherical ones. These differences suggest that Type-A CsMPs were formed through gas condensation, whereas Type-B CsMPs were formed through melt solidification. It is expected that (i) the ^{137}Cs concentration per volume of Type-A CsMP will be higher than that of Type-B CsMP, and (ii) that of spherical Type-B CsMP will be higher than that of nonspherical Type-B CsMP, since ^{137}Cs in Type-B CsMP is diluted by structural materials to a greater degree, particularly in nonspherical Type-B CsMP. These differences reflect the genetic processes of Type-A and two types of Type-B CsMPs.

To support the hypothesis, μ-XRF analysis was conducted particularly for rubidium (Rb) and strontium (Sr), since their X-ray fluorescence lines (Rb, Kα_1: 13.4 keV; Sr, Kα_1: 14.1 keV) were at high energies, which are not subject to the self-absorption effect. Since the matrix of CsMPs is SiO_2, the attenuation length was larger than 500 μm at X-ray energies above 13 keV. Therefore, Rb and Sr with high-energy XRF, which also represented volatile and refractory elements, respectively, were selected for the analysis. As expected from the volatility of these elements, spherical Type-B CsMPs had a higher Rb/Sr ratio than nonspherical Type-B CsMPs (Fig. 2). The Rb/Sr ratio in the spherical Type-B CsMPs increased with ^{137}Cs concentration, showing that spherical Type-B CsMPs have a higher concentration of volatile elements, including Cs, than nonspherical Type-B CsMPs. Similar results were also found for antimony-125 (^{125}Sb), another volatile radionuclide emitted from FDNPP.

Consequently, this study provided chemical and morphological characteristics of 67 CsMPs, the number of which is larger than in previous CsMP studies, which usually dealt with less than 10 particles. In addition, systematic variations found in the relationships of ^{137}Cs radioactivity with the (i) volume of CsMPs, (ii) porosity, (iii) Rb/Sr ratio, and (iv) ^{125}Sb activity allowed us to present some ideas regarding the formation and emission of CsMPs: (i) the condensation of gaseous species and melt solidification are the main processes for Types-A and -B CsMPs, respectively, and (ii) spherical particles had higher ^{137}Cs and ^{125}Sb concentrations and Rb/Sr ratios than nonspherical particles, possibly owing to the rapid cooling process, which inhibits the loss of volatile species during cooling.

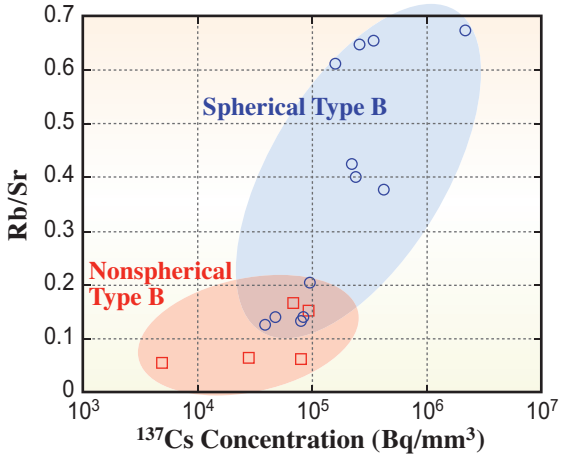

Fig. 2. Relationship between ^{137}Cs concentration and XRF intensity ratio of Rb/Sr for each CsMP.

Hikaru Miura[a] and Yoshio Takahashi[b,*]

[a] Atmospheric and Marine Environmental Sector, Central Research Institute of Electric Power Industry
[b] Department of Earth and Planetary Science, The University of Tokyo

*Email: ytakaha@eps.s.u-tokyo.ac.jp

References

[1] N. Yoshida and Y. Takahashi: Elements **8** (2012) 201.
[2] Y. Igarashi *et al.*: J. Environ. Radioactivity **205** (2019) 101.
[3] *H. Miura, Y. Kurihara, M. Yamamoto, A. Sakaguchi, N. Yamaguchi, O. Sekizawa, K. Nitta, S. Higaki, D. Tsumune, T. Itai and Y. Takahashi: Sci. Rep.* ***10*** *(2020) 11421.*
[4] H. Miura *et al.*: Geochem. J. **52** (2018) 145.
[5] Y. Kurihara *et al.*: Sci. Rep. **10** (2020) 3181.
[6] H. Miura *et al.*: Sci. Rep. **11** (2021) 5664.